

# Sharp vorticity gradients in two-dimensional hydrodynamic turbulence

E. A. Kuznetsov

*L.D. Landau Institute for Theoretical Physics,  
2 Kosygin str., 119334 Moscow, Russia*

V. Naulin, A. H. Nielsen, and J. Juul Rasmussen

*Optics and Plasma Research Department,  
OPL-128, Risø National Laboratory,  
P.O.Box 49, DK-4000 Roskilde, Denmark*

(Dated: 2004-07-16)

## Abstract

The appearance of sharp vorticity gradients in two-dimensional hydrodynamic turbulence and their influence on the turbulent spectra is considered. We have developed the analog of the vortex line representation as a transformation to the curvilinear system of coordinates moving together with the di-vorticity lines. Compressibility of this mapping can be considered as the main reason for the formation of the vorticity discontinuities at high Reynolds numbers. For two-dimensional turbulence in the case of strong anisotropy the vorticity discontinuities can generate spectra with the fall-off at large  $k$  proportional to  $k^{-3}$  resembling the Kraichnan spectrum for the enstrophy cascade. For turbulence with weak anisotropy the  $k$  dependence of the spectrum due to discontinuities coincides with that of the Saffman spectrum:  $k^{-4}$ . We have compared the analytical predictions with direct numerical solutions of the two-dimensional Euler equation for decaying turbulence. We observe that the di-vorticity is reaching very high values and is distributed locally in space along piecewise straight lines. Thus, indicating strong anisotropy and accordingly we found a spectrum close to the  $k^{-3}$ -spectrum.

## I. INTRODUCTION

This paper is concerned with investigations of two-dimensional (2D) hydrodynamical turbulent flows. In particular, we study the formation and dynamics of very sharp vorticity gradients and their influence on the energy spectrum in the enstrophy cascade regime. We may consider two kind of turbulent spectra. The first one was suggested by Kraichnan in 1967 [1], it corresponds to the enstrophy cascade directed to the small-scale region where viscous dissipation becomes essential. The Kraichnan spectrum follows, up to the logarithmic factor (see [2]), a power law for the scales intermediate between source and sink (the inertial interval):  $E(k) \sim \eta^{2/3}k^{-3}$  where  $\eta$  is the enstrophy dissipation rate. Recall that 2D turbulence additionally is characterized by an inverse energy cascade for large-scales leading to  $E(k) \sim k^{-5/3}$  (see e.g. [1]). However, in the present paper we will only be concerned with the small-scale region of the spectrum. The second spectrum suggested by Saffman in 1971 [3] yields another power dependence:  $E(k) \sim k^{-4}$ . According to Saffman, in decaying 2D turbulence vorticity discontinuities (in absence of viscosity) will form because fluid elements with different values of vorticity will be driven close together by the flow. Due to vorticity conservation the appearance of discontinuities will provide the conservation of all other invariants involving vorticity,  $\int \omega^n dS$ ,  $n = 3, 4, \dots$ . Accounting for a finite viscosity Saffman considers the "discontinuities" to have a small width  $\delta$ , which results from the balance between inertial and viscous forces. At high-Reynolds number this size is assumed to be very small in comparison with the length along the discontinuities,  $L$ , which may be assumed to be of the same order as the characteristic energy-containing length-scale. Under the assumption of isotropy and a dilute distribution of discontinuities Saffman suggested that the energy spectrum at large  $k$  could be constructed as a superposition of the spectra from the individual discontinuities resulting in:  $E(k) \sim k^{-4}$ .

From the first sight, the spectra obtained by Kraichnan and Saffman look like two different answers, but indeed, as we show in this paper, it is possible to establish some connection between them. This may be seen from the Fourier transform of a step function. Let us assume that the vorticity has a jump  $\Gamma = \Gamma(x)$  along the line  $y = 0$  and at first neglect effects connected with bending of the line. Then we can write:

$$\frac{\partial \omega}{\partial y} = \Gamma \delta(y).$$

Hence it is immediately seen that the Fourier transform will have a power-law fall-off at large

$k$ , i.e., inversely proportional to  $k_y$  multiplied by some function of  $k_x$  due to dependence of  $\Gamma$  on  $x$ . If we neglect the dependence on  $k_x$  replacing it by some constant, then we immediately obtain an energy spectrum with a power dependence similar to the Kraichnan spectrum:  $E(k) \sim k^{-3}$ . This is an important conjecture demonstrating that a spectrum similar to the Kraichnan spectrum, which is often observed in high resolution numerical simulations, may be related to discontinuities of vorticity which can be considered as possible candidates for singularities in ideal fluids in two dimensions. However, for viscous fluids, i.e., in the framework of the Navier-Stokes equation, such singularities are impossible: the initial smoothness of the solution will remain as proven first by Olga Ladyzhenskaya many years ago [4]. Within the 2D Euler equations for incompressible fluids the vorticity is a Lagrangian invariant and can never be singular, but its gradient might, in principle, become infinite in a finite time. Up to now this is an open question.

It is necessary to mention some examples of 2D flows presented by Yudovich [5], where the appearance of weaker singularities (vorticity is allowed to be discontinuous but bounded) are possible, however, they are formed in infinite time. Another approach based on the numerical analysis of the complex singularities for the inviscid flow with two-mode initial conditions showed that the width of its analyticity strip follows a  $\ln(1/t)$  law at short times [6, 7]. Additionally, many numerical experiments for 2D turbulence (see, [8]- [11]) show that with a good accuracy the Saffman spectrum is formed at the initial stage, before the excitation of the long-scale coherent vortices. The high-resolution numerical simulation performed by Legras et al. [12] demonstrated the power dependence  $k^{-3.5}$ . Analytical calculations presented by Gilbert [13] using arguments based on the existence of spiral structures give a power dependence with exponent between  $-3$  and  $-4$  (see also [14] and [15]). In particular, we would like to point to the very interesting paper by Ohkitani [16], where by means of the Weiss decomposition [17] it was shown that the so-called  $h$ -regions ( $h$ - hyperbolic in the sense of Ref. [17], i.e., regions where straining is dominating over vorticity) give the spectrum  $k^{-3}$ , i.e., coinciding up to a logarithmic factor with the Kraichnan spectrum, the contribution from the  $e$ -regions ( $e$ - elliptic, i.e., vorticity dominated regions) yield the Saffman spectrum  $\sim k^{-4}$ . Note, that similar ideas based on the wavelet analysis were developed in [18] to separate 2D turbulent flow into regions having different dynamical behaviors. The appearance of a power type spectrum in the short-wave region has been connected with different physical mechanisms like vortex merging [20], [21] and vortex stripping [22], [23] which give a certain

confirmation of the original idea of Saffman [3].

In this paper we present some qualitative physical arguments in favor of the formation of vorticity discontinuities in the 2D Euler equations for smooth initial conditions. The main idea in the description of 2D flows is connected with using the vorticity as Lagrangian invariants. Kuznetsov and Ruban [24] (see also [25]) developed a new kind of description for three-dimensional vortical flows - the so-called vortex line representation (VLR). This representation is based on the mixed Lagrangian-Eulerian description and connected with movable vortex lines. The VLR, which is a mapping to a curvilinear system of coordinates, turns out to be compressible, this is considered to be the main reason for breaking in hydrodynamics. Here we demonstrate how this approach can be modified for 2D Euler hydrodynamics. The main observation is that for 2D flows the curl of the vorticity, sometimes referred to as the di-vorticity [9, 16, 17], represents a frozen-in field, i.e., it satisfies the same equation as, e.g., the equation for the magnetic field in ideal 2D magneto-hydrodynamics (MHD). Therefore the generalization to the 2D Euler equations becomes straightforward. In the local case, as it was demonstrated for 2D MHD in Ref. [28], the vorticity plays the role of a Lagrangian coordinate and the other variable coincides with the Cartesian coordinate, say,  $x$ . In terms of these variables [28] the 2D Euler equations transform into equations of motion for a layered fluid, similar to stratified fluid, where each layer is labeled by its vorticity  $\omega$ . In terms of the new variables the "new" hydrodynamics becomes compressible. The derivative  $y_\omega$  plays the role of density of each layer, as a function of time and coordinate  $x$ . This characteristic is proportional to the width between two neighboring layers with closed vorticity contours.

Another aim of this paper is to revisit the energy spectra for 2D turbulence with emphasis on the angle distribution, following the arguments of Saffman connected with vorticity discontinuities. Using the stationary phase method we demonstrate that the contribution from one discontinuity is very anisotropic: it has a sharp angular peak along the direction perpendicular to the discontinuity. In the peak the energy spectrum falls-off like  $k^{-3}$  at large  $k$ . After average over angles in the case of isotropic turbulence the spectrum coincides with the Saffman spectrum [3].

In order to check whether the spectrum at large  $k$  is defined by vorticity discontinuities we have performed numerical experiments on decaying turbulence based on a direct numerical solution of the 2D Euler equations. In the turbulent state when the formation of power tails

is observed we examine the structure of the di-vorticity. We found that the di-vorticity is distributed very sharply in space concentrated on a random net of lines. In our opinion, these results can be interpreted in favor of the Saffman mechanism for the formation of 2D turbulent spectra due to discontinuities.

## II. TWO-DIMENSIONAL ANALOG OF THE VLR

Consider a 2D ideal fluid, described by the Euler equation for the vorticity  $\omega(x, y, t)$ ,

$$\frac{\partial \omega}{\partial t} + (\mathbf{v} \cdot \nabla)\omega = 0, \quad \text{div } \mathbf{v} = 0, \quad (1)$$

where the velocity field  $\mathbf{v}$  defines the vorticity:

$$\omega = \nabla \times \mathbf{v} = \frac{\partial v_y}{\partial x} - \frac{\partial v_x}{\partial y}.$$

Equation (1) shows that the vorticity is a Lagrangian invariant advected by the fluid, i.e.,

$$\omega(x, y, t) = \text{inv}$$

along a fluid particle trajectory defined as solution of the system of ordinary differential equations (ODE's),

$$\frac{d\mathbf{r}}{dt} = \mathbf{v}(\mathbf{r}, t), \quad \mathbf{r}|_{t=0} = \mathbf{a}. \quad (2)$$

Let us introduce the divergence-free vector field  $\mathbf{B}$  with the components

$$B_x = \frac{\partial \omega}{\partial y}, \quad B_y = -\frac{\partial \omega}{\partial x},$$

i.e.,  $\mathbf{B} = \text{curl } \omega \hat{z}$ . It is easily to see that this vector is tangent to the line  $\omega(x, y) = \text{const}$  because the vorticity gradient  $\nabla \omega = (\partial_x \omega, \partial_y \omega)$  is normal to this line. The equation of motion for the vector  $\mathbf{B}$  can be obtained from Eq. (1) after differentiating with respect to coordinates:

$$\frac{\partial \mathbf{B}}{\partial t} = \text{curl} [\mathbf{v} \times \mathbf{B}]. \quad (3)$$

Thus, the vector  $\mathbf{B}$  constitutes a frozen-in quantity. Sometimes, it is called as the di-vorticity (see [9]). By introducing the substantial (material) derivative,  $d/dt = \partial/\partial t + (\mathbf{v} \cdot \nabla)$ , Eq. (4) can be rewritten as

$$\frac{d\mathbf{B}}{dt} = (\mathbf{B} \cdot \nabla)\mathbf{v}. \quad (4)$$

Hence, we observe that  $|\mathbf{B}|$  will locally increase due to stretching of the di-vorticity lines, i.e., when

$$\frac{1}{2} \frac{d\mathbf{B}^2}{dt} = (\mathbf{B} \cdot \hat{S}\mathbf{B}) > 0, \quad (5)$$

where

$$\hat{S}_{ik} = \frac{1}{2} \left( \frac{\partial v_k}{\partial x_i} + \frac{\partial v_i}{\partial x_k} \right)$$

is the stress tensor. Increasing (or decreasing) the di-vorticity field, based on the equation (5), is not sufficient to clarify the physical mechanism for its growth. As is seen from Eq. (3) only one velocity component,  $\mathbf{v}_n$ , normal to the vector  $\mathbf{B}$  changes the field  $\mathbf{B}$ . In this case the tangential component  $\mathbf{v}_\tau$  (parallel to  $\mathbf{B}$ ) plays a passive role providing the incompressibility condition:  $\text{div } \mathbf{v}_\tau + \text{div } \mathbf{v}_n = 0$ . This observation is the key point for introducing the vortex line representation (VLR) for the three-dimensional Euler equations (see, e.g. [25]). To construct the analog of VLR for the 2D Euler equations we consider new Lagrangian trajectories, given by the  $\mathbf{v}_n$ ,

$$\frac{d\mathbf{r}}{dt} = \mathbf{v}_n(\mathbf{r}, t), \quad \mathbf{r}|_{t=0} = \mathbf{a}. \quad (6)$$

The solution of these ODE's defines a new mapping

$$\mathbf{r} = \mathbf{r}(\mathbf{a}, t) \quad (7)$$

which is different from that given by Eq. (2). In terms of this mapping the di-vorticity equation (3) can be integrated (for details see, e.g. [28]):

$$\mathbf{B}(\mathbf{r}, t) = \frac{(\mathbf{B}_0(\mathbf{a}) \cdot \nabla_a) \mathbf{r}(\mathbf{a}, t)}{J}, \quad (8)$$

where  $\mathbf{B}_0(\mathbf{a})$  is the initial di-vorticity,  $J$  is the Jacobian of the mapping (7):

$$J = \frac{\partial(x, y)}{\partial(a_x, a_y)}.$$

According to the definition of this mapping its Jacobian is not fixed, it may change in time and space. In other words, the mapping  $\mathbf{r} = \mathbf{r}(\mathbf{a}, t)$ , as a change of variables, represents a compressible mapping. This means that the di-vorticity lines can be compressed. In this approach the velocity of motion of di-vorticity lines is nothing else than the normal velocity  $\mathbf{v}_n$ .

It is interesting to note that this approach in slightly different form what was suggested in [28]. In this paper the basis of the approach is the mixed Lagrangian-Eulerian description

when all desired quantities are considered as functions of vorticity  $\omega$  (or any other Lagrangian invariant) and a Cartesian coordinate  $x$ .

The VLR given by (6), (7), (8) with the local change of variables  $\mathbf{r} = \mathbf{r}(\mathbf{a}, t)$ , does not work at singular points where the  $\mathbf{B}$ -field vanishes,

$$\mathbf{B}(\mathbf{r}(t), t) = 0. \quad (9)$$

and where, respectively, the normal velocity is not defined. For vorticity  $\omega$  these points are nothing more than maximal, minimal or saddle points. It is easy to see that the null points are advected by the fluid, but the velocity  $\mathbf{v}$  at these points is defined through the  $\mathbf{B}$ -field by inverting the Laplacian operator:  $\mathbf{v} = -\Delta^{-1}\mathbf{B}$ . The null-points for the normal vector field  $\mathbf{n}(\mathbf{r})$  represent topological singularities. Topological constraints as additional conditions to the system (6), (7), (8), are written as integrals of the vector field  $\mathbf{n}(\mathbf{r})$  along a loop enclosing the null-points:

$$\oint (\nabla\varphi \cdot d\mathbf{r}) = 2\pi m, \quad (10)$$

where  $\varphi$  is the angle between the vector  $\mathbf{n}$  and the  $x$ -axis and  $m$ , being a topological charge, is an integer equal to the total number of turns of the vector  $\mathbf{n}$  while passing around the closed contour with the null-point inside it (see also [28]). For instance, for  $X$ -points or  $O$ -points,  $m = \pm 1$ .

As well known from our knowledge in gas-dynamics compressibility of the mapping is a main cause for steepening and ultimately breaking, resulting in the formation of sharp gradients for the velocity and density of the gases. This happens in finite time and in the general situation the singularity first appears in one separate point, i.e., it may be related to collapse. In gas-dynamics this process is completely characterized by the mapping determined by the transition from the Eulerian to the Lagrangian description. Vanishing of the Jacobian corresponds to the emergence of a singularity. For three-dimensional incompressible Euler equations compressibility of the VLR is a possible reason for appearance of infinite vorticity in one separate point that results in breaking of vortex lines. The first study of vortex-line breaking for three-dimensional integrable hydrodynamics with the Hamiltonian  $\int |\omega| d\mathbf{r}$  was performed by Kuznetsov and Ruban [29]. Recent numerical experiments [26], [27] have confirmed the possibility of this type of scenario.

The Jacobian in denominator of the expressions (8) can become zero, which will result in infinite value of the di-vorticity. We do not see any restrictions by which this process can

be forbidden. In 2D hydrodynamics, however, compressibility of the mapping guarantees only compression of di-vorticity lines corresponding to the formation of sharp gradients for vorticity. Probably, the breaking process in 2D happens in infinite time (see, for instance, [5]). The most important point for us is that the tendency indeed does exist and it is possible to imagine that this process may be accelerated in the presence of external forces driving the turbulence.

### III. 2D SPECTRUM

In the previous section we gave some arguments in favor of formation of sharp gradients of the vorticity in 2D Euler flows. Everywhere below we will suppose that this process is possible and consider how it can effect the form of turbulent spectrum. For 2D turbulence, in the presence of finite viscosity and external forces, we will assume that the sharp vorticity gradients have a finite value inversely proportional to the characteristic width of discontinuity  $\delta$ , which is defined from the balance between inertial and viscous terms. At high Reynolds number the width  $\delta$  will be much less than the characteristic (energy-containing) scale  $L$ . In the turbulent state such discontinuities are naturally assumed to form a set of vorticity gaps with random positions of their centers, random forms and random distributions over angles. Our aim is to calculate the contribution to the spectrum from such discontinuities. We will be interested in the region of wave numbers  $k$  lying between  $L^{-1}$  and the inverse width  $\delta^{-1}$ :

$$L^{-1} \ll k \ll \delta^{-1}.$$

To simplify the problem all gaps are supposed to be concentrated on pieces of straight lines (finite intervals) with vorticity gaps vanishing at the endpoints of the intervals. As we will see later this simplification is not so essential. The answer, which we will get, will also account for bends of the discontinuity lines.

To find spectrum we need to calculate the Fourier transform from of pair correlation function:

$$F(\mathbf{r}) = \langle \omega(\mathbf{x})\omega(\mathbf{x} + \mathbf{r}) \rangle,$$

where angle brackets means average over the ensemble of discontinuities. Hence the energy

density spectrum  $\epsilon(\mathbf{k})$  is given by the standard formula:

$$\epsilon(\mathbf{k}) = \frac{F_k}{2k^2} = \frac{\overline{|\omega_k|^2}}{8\pi^2 S k^2}$$

where  $\omega_k$  is the Fourier transform of the vorticity  $\omega(\mathbf{r})$ ,

$$\omega_k = \int \omega(\mathbf{r}) e^{-i(\mathbf{k}\mathbf{r})} d\mathbf{r}, \quad \omega(\mathbf{r}) = \frac{1}{(2\pi)^2} \int \omega_k e^{i(\mathbf{k}\mathbf{r})} d\mathbf{k},$$

the over-bar denotes average with respect to random variables, and  $S$  is the average area, which is assumed to be sufficiently large.

Consider first one discontinuity with the center at  $\mathbf{r}_0 = (x_0, y_0)$  oriented along the  $y$ -axis. Then for the  $y$ -derivative of  $\omega$  we have,

$$\frac{\partial \omega}{\partial y} = \Gamma(x) \delta(y - y_0) + \text{regular terms.} \quad (11)$$

Here  $\Gamma(x)$  is a continuous function of  $x$  inside the interval  $[x_1, x_2]$  vanishing at the endpoints  $x = x_{1,2}$  and equal zero outside the interval.

Hence, the Fourier transform from the singular part of  $\omega$  is given by the integral:

$$\omega_k = -\frac{i}{k_y} e^{-ik_y y_0} \int_{x_1}^{x_2} \Gamma(x) e^{-ik_x x} dx$$

where  $\mathbf{k} = (k_x, k_y)$ . This is the contribution from one discontinuity. If we assume that the discontinuities are not very densely distributed, they may be considered "independent" and the spectrum for the whole ensemble of discontinuities may be obtained by a superposition of the spectra from the individual discontinuities, i.e., from the summation with respect to all discontinuities which results in

$$\omega_k = -\sum_{\alpha} \frac{i}{(\mathbf{k} \cdot \mathbf{n}_{\alpha})} e^{-i(\mathbf{k} \cdot \mathbf{n}_{\alpha}) y_{0\alpha}} \int_{x_{1\alpha}}^{x_{2\alpha}} \Gamma_{\alpha}(x) e^{-i(\mathbf{k} \cdot \boldsymbol{\tau}_{\alpha}) x} dx. \quad (12)$$

Here we have introduced two unit vectors: normal  $\mathbf{n}_{\alpha}$  and tangent  $\boldsymbol{\tau}_{\alpha}$  ( $\mathbf{n}_{\alpha}^2 = \boldsymbol{\tau}_{\alpha}^2 = 1$ ,  $(\mathbf{n}_{\alpha} \boldsymbol{\tau}_{\alpha}) = 0$ ) characterizing the orientation of the  $\alpha$ -th discontinuity. The coordinates  $x_{1\alpha}, x_{2\alpha}, y_{0\alpha}$  together with the two unit vectors define completely the positions of the discontinuities.

To find an enstrophy spectrum one needs to perform average of  $|\omega_k|^2$  with respect to all random variables. Assuming the coordinates of the discontinuities to be randomly distributed uniformly in space, the first average gives:

$$\overline{|\omega_k|^2} = N \left\langle \frac{1}{(\mathbf{k} \cdot \mathbf{n})^2} \left| \int_{x_1}^{x_2} \Gamma(x) e^{-i(\mathbf{k} \cdot \boldsymbol{\tau}) x} dx \right|^2 \right\rangle. \quad (13)$$

Here  $N$  is the number of discontinuities in area  $S$ , angle brackets means the average with respect to both  $x_1, x_2$  and angle distribution.

Since we are interested in short-wave asymptotics of the spectrum,  $kL \gg 1$ , the integrand in (13) in this case represents a rapidly varying function of  $x$ . Therefore the integral in (13) can be estimated by means of the method of stationary phase. This method can be applied for all angles except for a narrow cone of angles,  $\theta_k$  ( $\theta_k$  is the angle between the vectors  $\mathbf{n}$  and  $\mathbf{k}$ ) where  $kL\theta_k \leq 1$ . In this region the integral can be considered as constant which results in the following form for the energy distribution (before angle averaging!):

$$\epsilon_1(\mathbf{k}) \approx \frac{n}{8\pi^2 k^4} \langle (\bar{\Gamma}l)^2 \rangle, \quad \theta_k \leq \theta_0 \equiv (kL)^{-1}, \quad (14)$$

where  $n$  is the density of discontinuities ( $= N/S$ ) and

$$\bar{\Gamma}l = \int_{x_1}^{x_2} \Gamma(x) dx, \quad l = x_2 - x_1, \quad \langle l \rangle = L.$$

For angles  $\theta_k$  lying far from  $\theta_0 \equiv (kL)^{-1}$  the integral in (13) can be estimated by means of the method of stationary phase. However, the leading order, proportional to  $(\mathbf{k}\tau)^{-1}$ , gives zero input because  $\Gamma(x_{1,2}) = 0$ . Therefore one needs to keep the next order approximation that gives:

$$\epsilon_2(\mathbf{k}) \approx \frac{N}{4\pi^2 k^2} \frac{\langle (\Gamma')^2 \rangle}{(\mathbf{k} \cdot \mathbf{n})^2 (\mathbf{k} \cdot \boldsymbol{\tau})^4}, \quad \theta_k \gg (kL)^{-1}, \quad (15)$$

where  $\Gamma'$  is the derivative of  $\Gamma$  taken at the endpoints  $x_i$ . This formula demonstrates singular behavior for  $\epsilon(\mathbf{k})$  at angles  $\theta_k$  close to 0 and  $\pi/2$  (as well as, to  $\pi$  and  $-\pi/2$ ). At small angles  $\theta_k \leq (kL)^{-1}$  this expression has to be matched with (14). For the angle range close to  $\pi/2$  the integral in (15) should be cut-off due to the bending of the line of discontinuity. This factor switches on at angles  $|\theta_k - \pi/2| \sim (ka)^{-1}$  where  $a$  is a characteristic bending length of discontinuity (roughly of the order of  $L$ ). Thus, the energy density distribution  $\epsilon(\mathbf{k})$  has a very narrow angle maximum at  $\theta_k$  near zero with decay at large wave numbers as  $\sim k^{-4}$ , this results in the energy spectrum  $E(k) \sim k^{-3}$ , which, up to the logarithmic factor, corresponds to the Kraichnan spectrum. For all other angles  $\epsilon(k)$  decays proportionally to  $k^{-6}$  at large  $k$ .

We would like to stress once more that the formulas (14) and (15) are the results of non-complete average, i.e, the average with respect to coordinates  $x_{1\alpha}, x_{2\alpha}, y_{0\alpha}$ . In order to get the final answer for the energy spectrum it is necessary to average with respect to angles.

Let us assume first that the angle distribution is isotropic. Then, integrating over angles it is easily seen that from the first region (14) we have the following contribution:

$$E_1(k) = 2k \int_{-\theta_0}^{\theta_0} \epsilon_1(k) d\theta_k \approx \frac{n}{2\pi^2 k^4 L} \langle (\bar{\Gamma}l)^2 \rangle. \quad (16)$$

Here the factor 2 appears because of two equal contributions from two regions near  $\theta_k = 0$  and  $\theta_k = \pi$ . Averaging (15) over angles gives divergence at  $\theta \rightarrow 0$  and  $\theta \rightarrow \pi/2$ . The main contribution to the energy spectrum comes from the cut-off at small angles  $\sim (kL)^{-1}$ :

$$E_2(k) \approx \frac{nL^3}{3\pi^2 k^4} \langle (\Gamma')^2 \rangle. \quad (17)$$

Thus, both regions of angles give contributions of the same order of magnitude. The complete answer for the energy spectrum for isotropic turbulence (i.e., isotropic distribution of discontinuities) is given by the sum of (16) and (17):

$$E(k) \approx \frac{n}{2\pi^2 k^4 L} \left[ \langle (\bar{\Gamma}l)^2 \rangle + \frac{2L^4}{3} \langle (\Gamma')^2 \rangle \right], \quad (18)$$

which coincides with the spectrum obtained by Saffman [3].

In order to find the spectrum in the anisotropic situation one needs to average expressions (14), (15) with the corresponding distribution function. In numerical experiments anisotropy can be conditioned by box boundaries as well as by anisotropy of the pumping of turbulence. In the case when such ordering is strong enough the spectrum may get some peculiarities originating from non-averaged spectra given by (14), (15). If the width of the angle distribution function  $\Delta\theta$  will be narrower than  $\theta_0 = (kL)^{-1}$ , then in the angle cone  $\theta_k < \Delta\theta$  the energy spectrum  $E(k, \theta)$  will have the fall-off  $\sim k^{-3}$ , i.e., the same power dependence as for the Kraichnan spectrum. Note, however, that this asymptotics is only intermediate because  $\theta_0 = (kL)^{-1}$  decreases with increasing  $k$ . Therefore starting from  $k = k^* = (L\theta_0)^{-1}$ , the average over angles becomes sensitive relative to the singularities of (15) that results in the spectrum decreasing proportional to the Saffman fall-off. If the influence of anisotropy is not so essential then we should expect the spectrum close to the Saffman one, of course, in the case when the main contribution to the spectrum at large  $k$  is connected with discontinuities. The most interesting observation following from the analytical results of this Section is that in the very anisotropic case with strong ordering of discontinuities the sharp angular maximum of the spectrum has the power fall-off coinciding with that for the Kraichnan spectrum. While in the isotropic case our answer coincides with the Saffman answer. In the

next Section we present the results of numerical simulation of decaying 2D turbulence at high-Reynolds numbers. In particular, the appearance of the power law tails in the energy spectrum at large  $k$  can be explained rather by discontinuities, than by a cascading process with constant enstrophy.

#### IV. NUMERICAL INVESTIGATIONS

To support the arguments of the previous sections and reveal the direct connection between the formation of the sharp vorticity gradients and the tail of the energy spectrum we have performed a numerical study of the evolution of decaying 2D turbulence. The 2D Euler equations (1) in the vorticity-streamfunction formulation are integrated numerically on a double periodic domain by employing a high resolution fully de-aliased spectral scheme:

$$\frac{\partial \omega}{\partial t} + \{\omega, \psi\} = \mu_{2n} \nabla^{2n} \omega, \quad (19)$$

where  $\psi$  is the streamfunction related to the vorticity by the Poisson equation:  $\omega = -\nabla^2 \psi$ , the velocity is given as  $\mathbf{v} = (v_x, v_y) = \nabla \psi \times \hat{z}$  and the bracket

$$\{\omega, \psi\} \equiv \mathbf{v} \cdot \nabla \omega = \frac{\partial \omega}{\partial x} \frac{\partial \psi}{\partial y} - \frac{\partial \psi}{\partial x} \frac{\partial \omega}{\partial y}.$$

In solving (19) we have included a hyperviscosity term on the right hand side of the equation to keep the integration scheme stable (typically we have used  $n = 3$  and  $\mu_6 = 10^{-20}$ ). This term was observed to decrease the energy by less than 0.002% and the enstrophy by less than 20%. We verified that the global features of our results were not dependent on the type of viscosity (alternatively we used kinematic viscosity). In the present context we apply the hyperviscosity to allow an as wide a dynamical range as possible with the given resolution. The domain size is taken to be unity and the resolution is  $2048 \times 2048$  modes. For the time integration we employ a third order stiffly-stable scheme. We have chosen the time scale to correspond to  $\omega_0^{-1}$ , where  $\omega_0$  corresponds to the maximum vorticity.

As initial condition we have placed a number of positive and negative vortices randomly on the domain, ensuring that the total circulation is zero. Vortices of various shapes/profiles from vortex patches (Rankine vortices) to Gaussian vortices form the initial condition. In the simulation run described here, we have thus used 10 vortices of each sign with Gaussian profiles:

$$\omega(r, \theta) = \pm \omega_0 \exp(-r^2/R_0^2), \quad (20)$$

where  $\omega_0 = 1$  for all vortices, while their radii  $R_0$  are varying in the range  $0.02 < R_0 < 0.075$ . In Fig. 1a we show the initial vorticity field and Fig. 1b the vorticity field at  $T = 95$ , which corresponds to around 8 vortex internal turnover times ( $T_v \equiv 4\pi/\omega_0$ ). The vorticity field has the typical structure for 2D turbulence; it consist of large scale structures (vortices) with concentrated vorticity and strongly filamented structures between the vortices. At this time there is still strong dynamics in the flow evolution, with shearing and straining due to mutual interactions of nearby structures. Corresponding to the vorticity field we show the instantaneous one-dimensional energy spectrum  $E(k)$  (total energy:  $E = \int_0^\infty E(k)dk$ ) in Fig. 2. The spectrum  $E(k)$  for  $T = 0$  in Fig. 2 shows the spectrum of superimposed Gaussian vortices. The spectrum is expanding to the high  $k$ -values and at  $T = 95$  a  $k^{-\alpha}$  spectrum is developed at high wavenumbers for the present case  $\alpha \sim 3$ , as clearly demonstrated in Fig. 2, which show the compensated spectrum  $k^3 E(k)$  being constant over almost 2 decades in  $k$ .

To investigate the details of the dynamics and how the  $k^{-\alpha}$  spectrum is generated, we plot in Fig. 3 the di-vorticity field  $\mathbf{B}$  defined in Sec. II, showing the length  $|\mathbf{B}|$ , which is equal to  $|\nabla\omega|$ . It is clear from the figure that very sharp vorticity gradients appears. These are localized in stripes that are mostly along straight lines. The stripes are mainly formed outside the dominating vortex structures, and their formation can be explained by the analysis discussed in Sec. II. Furthermore it is evident that the concentration of the stripes are relatively low. Following the time evolution of maximum value of  $|\mathbf{B}|$ ,  $B_{max}$ , we observe a very rapid growth to values more than 100 times the initial value.  $B_{max}$  oscillates in time with a typical period related to the vortex turnover time,  $T_v$ . The highest maximum reached during this simulation approach 1000, which with a maximum value of the vorticity  $\omega_0 = 1$  corresponds to the width of the filaments  $\delta < 0.001$ , it is evident that the growth of  $|\mathbf{B}|$  is arrested by the hyperviscosity, and indeed  $B_{max}$  scales with  $\mu_6^{-1/6}$ . We compare the structure of the di-vorticity field with the high pass filtered vorticity field shown in Fig. 4. The very similar structure of the high pass filtered vorticity field and the vorticity gradient field strongly suggests that the vorticity gradients are responsible for the large- $k$  part of the spectrum, i.e., the  $k^{-\alpha}$  part.

To further discuss the dynamics we show the Weiss field [17] in Fig. 5, defined by  $W =$

$\frac{1}{4}(s^2 - \omega^2)$  where

$$s = [(\frac{\partial v_x}{\partial x} - \frac{\partial v_y}{\partial y})^2 + (\frac{\partial v_y}{\partial x} + \frac{\partial v_x}{\partial y})^2]^{1/2}$$

is the rate of deformation. Comparing Figs. 3 and 5 we observe that the vorticity gradient stripes are aligned with the contours of  $W$  in the strain dominated regions,  $W > 0$ , mainly at the edge of the vortex structures and in between the structure. A careful inspection, however, reveals that in the stripes  $W < 0$ , i.e., vorticity dominates. This is in line with the original arguments of Weiss (see also [16, 19]) that vorticity gradients will tend to concentrate in the strain dominated regions. In particular in the work of Chen *et al.* [19] it was demonstrated that the dynamics leading to the enstrophy cascade in driven 2D turbulence is most significant in strain dominated regions.

The spectra we have observed is characterized by having the exponent close to  $\alpha = 3$ . Thus, with reference to Sec. III this will correspond to the spectrum in the anisotropic regime where the stripes of vorticity gradients are near straight lines. Indeed in Fig. 3 we see that we have stripes that are close to straight lines and the observed spectrum is this in keeping with the expectations. To illustrate the anisotropic nature of the spectrum directly we plot in Fig. 6 the two dimensional spectrum,  $\epsilon(k_x, k_y)$ . We observe a clear anisotropy, which become particular apparent in the compensated spectrum in Fig. 6b, which is obtained by subtracting the angle average of  $\epsilon(k_x, k_y)$  (i.e.,  $(2\pi)^{-1} \int_0^{2\pi} \epsilon(k_x, k_y) d\theta$ ). Here we observe a clear angular structure. We should emphasize that the spectra obtained here are instantaneous spectra obtained a one time and for one realization. Ensemble averaged spectra are expected to show a much higher degree of – if not complete – angle isotropy.

## V. CONCLUDING REMARKS

We have performed a detailed investigation of the relation between turbulent spectra and possible singularities in 2D turbulent flows. First, we have demonstrated that the  $k$ -behavior of the spectra generated by sharp vorticity gradients, based on the compressible advection of di-vorticity, depends significantly on the anisotropy of the spectra. If the angular spectrum distribution has one or more very sharp peaks then the one-dimensional spectrum has a tail falling-off like  $k^{-3}$  at large  $k$ , which is resembling the Kraichnan spectrum, derived from spectral cascade arguments. In the opposite case of an isotropic smooth angular dependence the spectrum has an asymptotic behavior  $k^{-3}$  as for the Saffman spectra. These arguments

allow us to suggest interpretation of many numerical experiments where the spectral exponent varies in the whole interval between  $-3$  and  $-4$ . For instance, in the simulations by Okhitani [16] the  $e$ -regions, because of their geometry, would give the main contributions to the isotropic component of the spectrum which explain the Saffman exponents for the observed spectrum in [16]. For  $h$ -regions the situation is different: these regions contain stretched vorticity level lines and their contribution to the spectrum should be expected to be very anisotropic. This is why these regions produce the  $k$ -behavior as for the Kraichnan spectrum. A similar situation takes place in our simulations in comparison with the numerics performed before [20, 21]. In the both latter simulations the spectra were isotropic resulting in spectral exponents like for the Saffman spectrum. In the simulations presented in the present paper we have very strong vorticity gradients concentrated on the very narrow stripes and therefore the exponent is close to that for the Kraichnan spectrum. Employing a filtering of the vorticity field indicates, more or less one-to-one, that the tail of the spectrum originates from the sharp vorticity gradients. A strong amplification of di-vorticity of more than hundred times is one of the main results of our simulations. A detailed investigation of the growth of the di-vorticity maximum is beyond the main scope of this paper and will be considered in future works. In conclusion, we stress that this amplification has a natural explanation due to compressibility of the mapping (7) providing the transfer from the Eulerian description to the system of movable curvilinear di-vorticity lines as described in Sec. II.

## VI. ACKNOWLEDGMENTS

This work was supported by INTAS (grant no. 00-00292). The work of E.K. was also supported by the RFBR (grant no. 00-01-00929). E.K. wishes to thank Riso National Laboratory, where this work was initiated, for its kind hospitality during the visit in November, 2003. JJR thanks the Landau Institute for kind hospitality during a visit in June 2004, where the work was finalized.

---

[1] R.H. Kraichnan, Phys. Fluids **11**, 1417 (1967).

[2] R.H. Kraichnan, J. Fluid Mech. **47**, 525 (1971); J. Fluid Mech. **62**, 305 (1974).

- [3] P. G. Saffman, *Stud. Appl. Maths* **50**, 49 (1971).
- [4] O.A. Ladyzhenskaya. *The mathematical theory of viscous incompressible flow*, Gordon and Breach, 1969.
- [5] V.I. Yudovich, *Zh. Vychisl. Mat. Mat. Fiz.*, **3**, 1032 (1963); *Chaos*,**10**, 705 (2000).
- [6] U. Frisch, T. Matsumoto and J. Bec, *J. Stat. Phys.* **113**, 761 (2003).
- [7] T. Matsumoto, J. Bec, and U. Frisch, *Fluid Dyn. Res. in Press* (2004) (arXiv:nln.CD/0310044 v2 1 Apr 2004.)
- [8] J.C. McWilliams, *J. Fluid Mech.*, **146**, 21 (1984).
- [9] S. Kida, *J. Phys. Soc. Jpn.* **54** 2840 (1985).
- [10] M.E. Brachet, M.Meneguzzi, P.L. Sulem, *Phys. Rev. Lett.* **57**, 683 (1986).
- [11] R. Benzi, S. Patarnello, P. Santangelo, *Europhys. Lett.* **3**, 811 (1986).
- [12] B. Legras, B. Santangelo, R. Benzi, *Europhys. Lett.* **5**, 37 (1988); B. Santangelo, R. Benzi, and B. Legras, *Phys. Fluids A* **1**, 1027 (1989).
- [13] A.D. Gilbert, *J. Fluid Mech.*, **193**, 475 (1988).
- [14] H.K. Moffatt, *Spiral structures in turbulent flow*, in *New Approaches and Concepts in Turbulence*, eds. Th. Dracos and A. Tsinober (Birkhäuser, Basel, 1993) p. 121.
- [15] J.C. Vasilicos, and J.C.R. Hunt, *Proc. R. soc. Lond. A* **435**, 505 (1991).
- [16] K. Okhitani, *Phys. Fluids A* **3**, 1598 (1991).
- [17] J. Weiss, La Joila Institute Report No. LJ1-TN-81-121, 1981; *Physica D* **48**, 273 (1991).
- [18] M. Do-Khaca, C. Basdevant, V. Perrierd and K. Dang-Tranc, *Physica D*, **76**, 252 (1994).
- [19] S. Chen, R.E. Ecke, G.L. Eyink, X. Wang and Z. Xiao, *Phys. Rev. Lett.* **91**, 214501 (2003).
- [20] A.H. Nielsen, X. He, J.J. Rasmussen, and T. Bohr, *Phys. Fluids*, **8**, 2263 (1996).
- [21] J.J. Rasmussen, A.H. Nielsen and V. Naulin, *Phys. Scripta*, **98**, 29-33 (2002).
- [22] D.G. Dritschel, *Phys. Fluids A* **5**, 984 (1993); *J. Fluid Mech.* **293**, 269 (1995).
- [23] B. Legras and D. Dritschel, *Applied Scientific Research*, **51**, 445-455, in *Advances in Turbulence IV*, Ed. F.T.M. Neiuwstadt, Kluwer, 1993.
- [24] E.A. Kuznetsov and V. P. Ruban, *JETP Letters*, **67**, 1076 (1998); *Phys. Rev. E*, **61**, 831 (2000).
- [25] E.A. Kuznetsov, *Pis'ma v ZHETF*, **76**, 406 (2002) [*JETP Letters*, **76**, 346 (2002)]; physics/0209047.
- [26] V.A. Zheligovsky, E.A. Kuznetsov, and O.M. Podvigina, *Pis'ma v ZhETF* **74**, 402 (2001)

- [JETP Letters, **74**, 367 (2001)].
- [27] E. A. Kuznetsov, O.M.Podvigina, and V.A.Zheligovsky, FLUID MECHANICS AND ITS APPLICATIONS, Volume 71: Tubes, Sheets and Singularities in Fluid Dynamics. eds. K. Bajer, H.K. Moffatt, Kluwer, (2003) pp. 305-316; physics/0110046.
- [28] E.A. Kuznetsov, T. Passot, P.L. Sulem, Phys. Plasmas **11**, 1410 (2004); physics/0310006.
- [29] E.A. Kuznetsov, V.P.Ruban, ZhETF **118**, 893 (2000) [JETP **91**, 776 (2000)].

## Figures

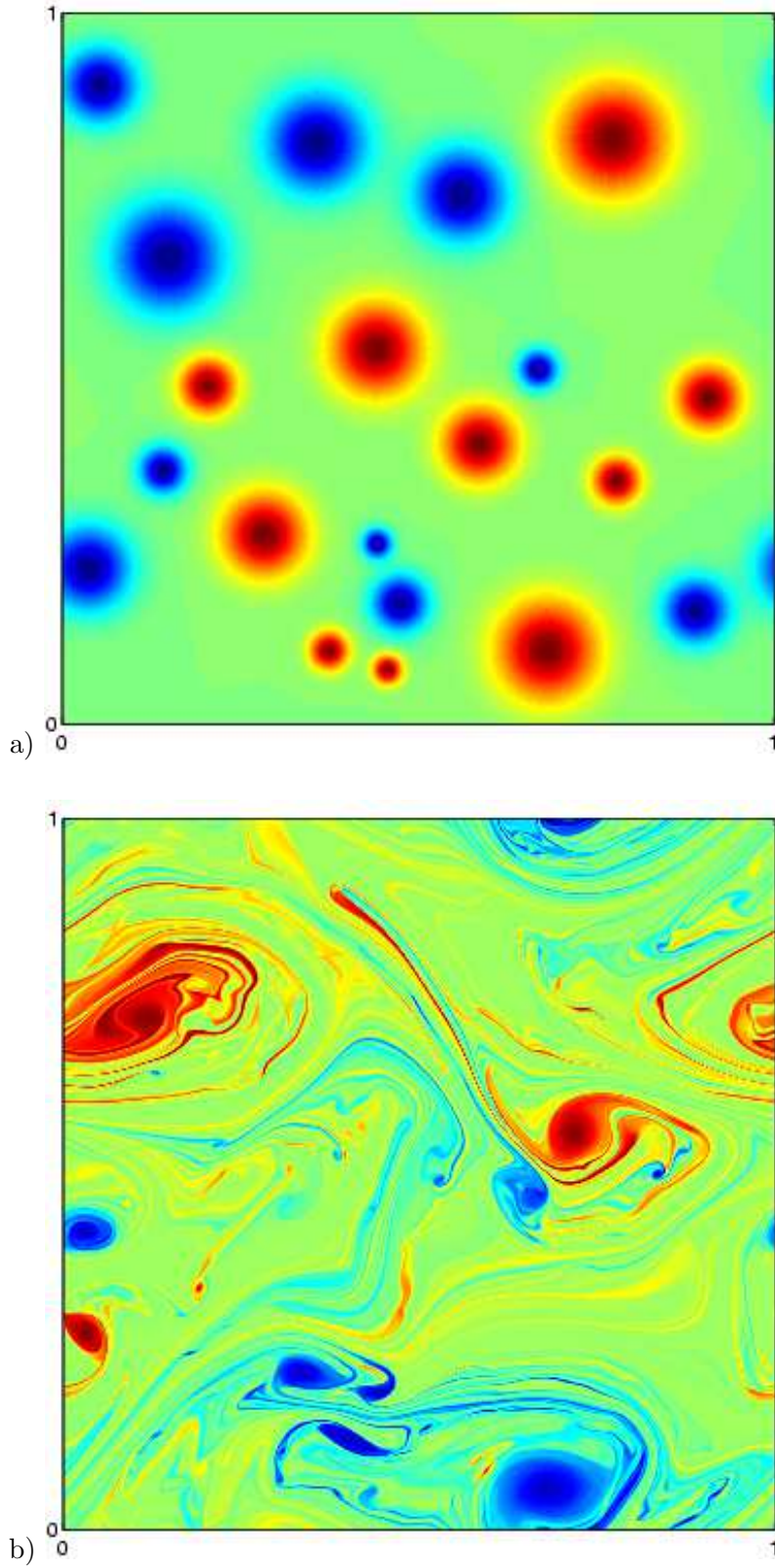


FIG. 1: a) Initial vorticity field. b) Vorticity field at time 95 corresponding to 10 vortex turnover times. Red color designates positive vorticity and blue color negative vorticity; maximum value is 1 and minimum value is -1.  $\omega_0 = 1$

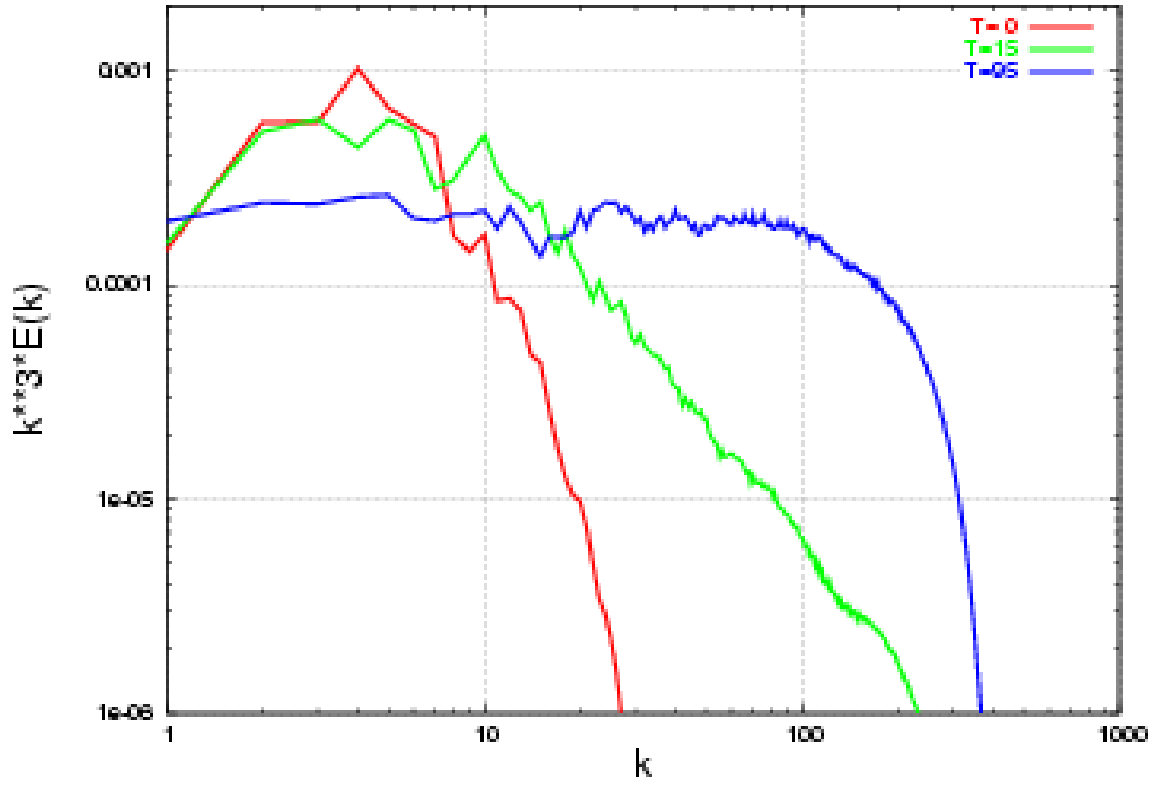


FIG. 2: Compensated energy spectrum at different times  $k^3E(k)$  corresponding to the vorticity field shown in Fig. 1.

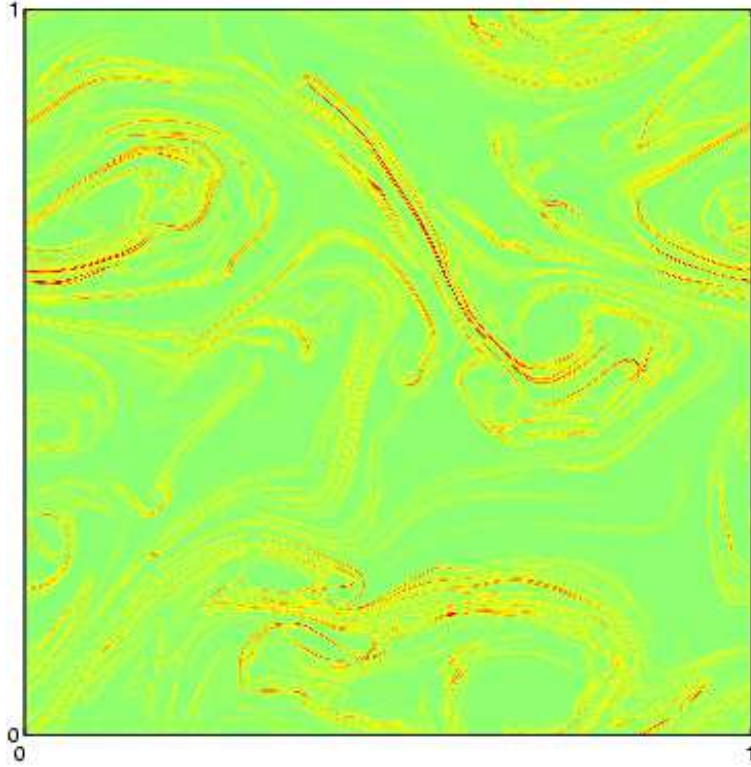


FIG. 3: The di-vorticity field  $\mathbf{B}$  at  $T = 95$ . Here the length of di-vorticity vector with the maximum (red) value being 673.

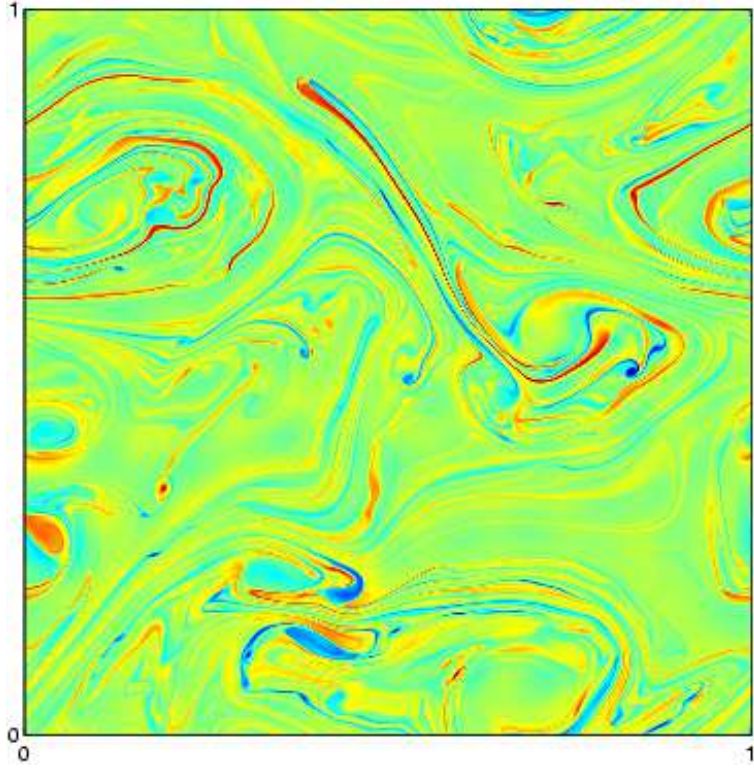


FIG. 4: High pass filtered vorticity field from Fig. 1b,  $k > 10$ .

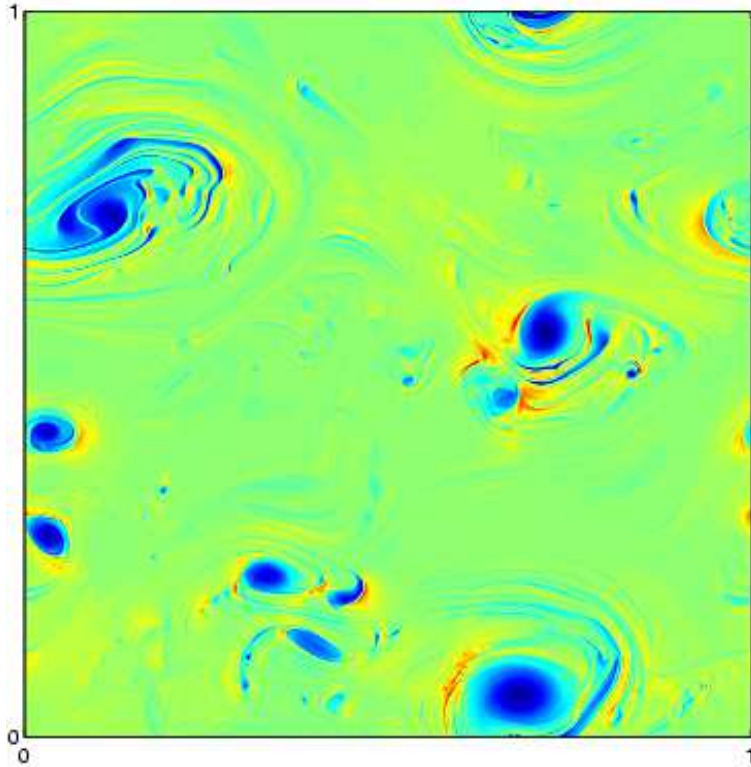
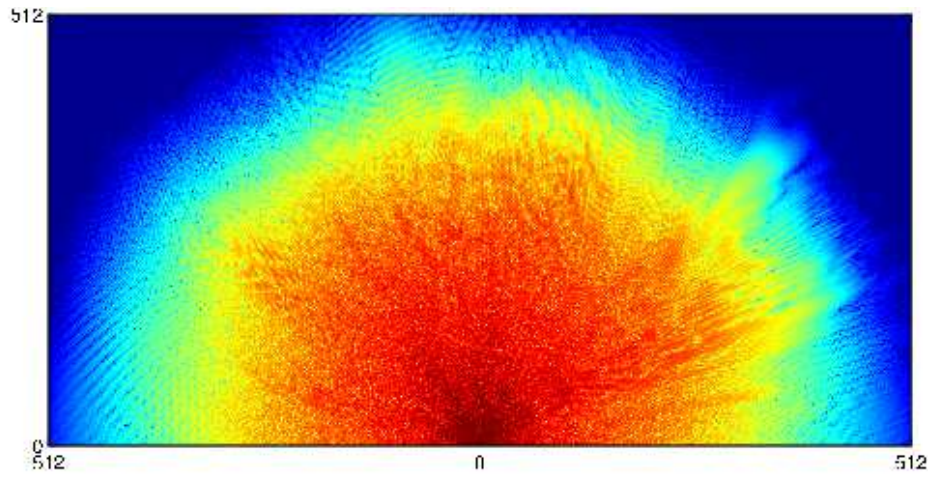
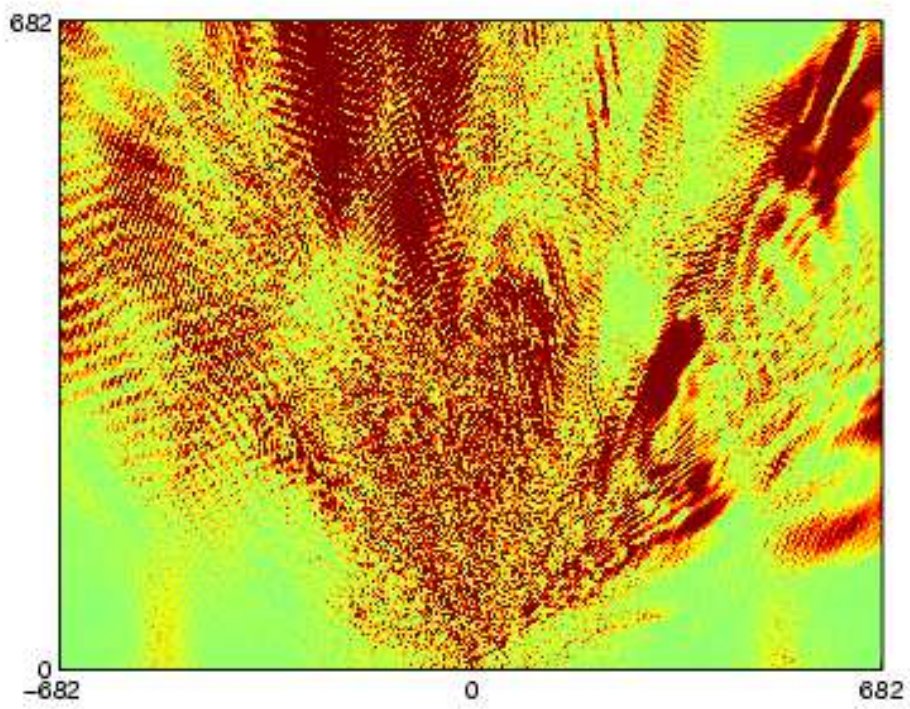


FIG. 5: Weiss field for the vorticity field show in Fig. 1b. Red designates positive values, i.e., strain dominated regimes. Blue designates negative values, i.e., vorticity dominated regimes.



a)



b)